ON MICRO-TO-MACRO CONNECTIONS IN STRONG COUPLING MULTISCALE MODELING OF SOFTENING MATERIALS

O. LLOBERAS-VALLS[*], D. J. RIXEN[†], A. SIMONE[*] AND L. J. SLUYS[*]

[*]Faculty of Civil Engineering and Geosciences
Delft University of Technology
P.O. Box 5048, 2600 GA Delft, The Netherlands
e-mail: O.LloberasValls@tudelft.nl

[†]Faculty 3mE
Delft University of Technology
Mekelweg 2, 2628 CD Delft, The Netherlands

Key words: Concurrent multiscale analysis, micro-to-macro connection, FETI, strain localization and softening

Abstract. In this contribution we describe a methodology for the multiscale analysis of heterogeneous quasi-brittle materials. The algorithm is based on the finite element tearing and interconnecting FETI [1] method cast in a non-linear setting. Adaptive multiscale analysis is accounted for with the use of selective refinement at domains that undergo non-linear processes. We focus on the micro-to-macro connection method which constitutes the strategy to handle incompatible interfaces arising from the connection of non-matching meshes. The behaviour of standard collocation and average compatibility techniques is assessed for a multiscale analysis of damage propagation in a quasi- brittle material. The choice of the connection strategy has an influence on the overall response and the computational cost of the analysis.

1 INTRODUCTION

The adopted methodology to enforce interscale relations in multiscale analysis certainly influences the overall mechanical response. Early examples of interscale relations in multiscale approaches are found in classical homogenization theory [2]. In this context, closed-form expressions are derived in order to synthesize effective properties from a heterogeneous microstructure. Examples of such techniques constitute the constant strain and stress assumptions at the microscale. Such assumptions, in combination with Hill's energy condition [3], lead to the well known Voigt and Reuss bounds. The study of complex microstructures undergoing non-linear behaviour has resulted in more sophisticated

homogenization techniques. In many cases, a closed-form expression can not be explicitly derived, however, numerical and computational homogenization techniques [4, 5, 6] are used to synthesize "on the fly" the constitutive behaviour of a representative microstructural sample. Constant strain and stress assumptions together with periodic conditions are well established micro-to-macro transition strategies which evolve from the earlier classical homogenization theory.

Similar strategies concerning interscale relations can be employed in concurrent multiscale techniques [7, 8, 9]. In these methodologies, coarse and fine scale regions are processed simultaneously. Hence, interscale constraints are designed to connect two incompatible meshes. The simplest choice corresponds to the well established collocation technique. Several weak versions of the collocation approach are represented by the family of mortar methods [10, 11]. Their effect in the multiscale analysis of elastic large scale structural analysis has been investigated in [12]. However, the influence of such constraints on the adaptive multiscale analysis of damage growth is accounted for in the present study.

2 MULTISCALE APPROACH

The multiscale approach adopted in this manuscript is based on an extension of the FETI framework presented in [13]. Below, the basic formulation and the adaptive multiscale features are summarized for completeness.

2.1 Basic formulation

Consider a body Ω with heterogeneous underlying structure and boundary conditions depicted in Figure 1. The body Ω is divided into N_s non-overlapping domains $\Omega^{(s)}$ connected by the interface Γ_I.

In a general concurrent multiscale analysis, where coarse (c) and fine (f) material resolutions co-exist, the resulting interface satisfies $\Gamma_\mathrm{I} = \Gamma_\mathrm{I}^\mathrm{cc} \cup \Gamma_\mathrm{I}^\mathrm{ff} \cup \Gamma_\mathrm{I}^\mathrm{cf}$, where the superscripts denote coarse to coarse mesh connection (cc), fine to fine mesh connection (ff) and coarse to fine mesh connection (cf). Note that in the present approach $\Gamma_\mathrm{I}^\mathrm{cc}$ and $\Gamma_\mathrm{I}^\mathrm{ff}$ are conforming whereas $\Gamma_\mathrm{I}^\mathrm{cf}$ is non-conforming except for the common nodes. These nodes are referred to as independent since they all meet a corresponding pair at the adjacent mesh. Dependent nodes are found at the non-conforming interfaces $\Gamma_\mathrm{I}^\mathrm{cf}$ and their nodal solution can be expressed as a function of the solution field at independent nodal points.

Continuity of the incremental solution field $\delta\mathbf{u}$ at the interface Γ_I between two different adjacent domains s and p reads

$$\delta\mathbf{u}^{(s)} = \delta\mathbf{u}^{(p)} \quad \text{at } \Gamma_\mathrm{I}, \tag{1}$$

and is satisfied with the introduction of linear multipoint constraints (LMPC). The set of LMPC is cast in a matrix form using modified Boolean matrices $\bar{\mathbf{B}}^{(s)}$. These matrices are constructed by row-wise concatenation of the tying relations between independent and
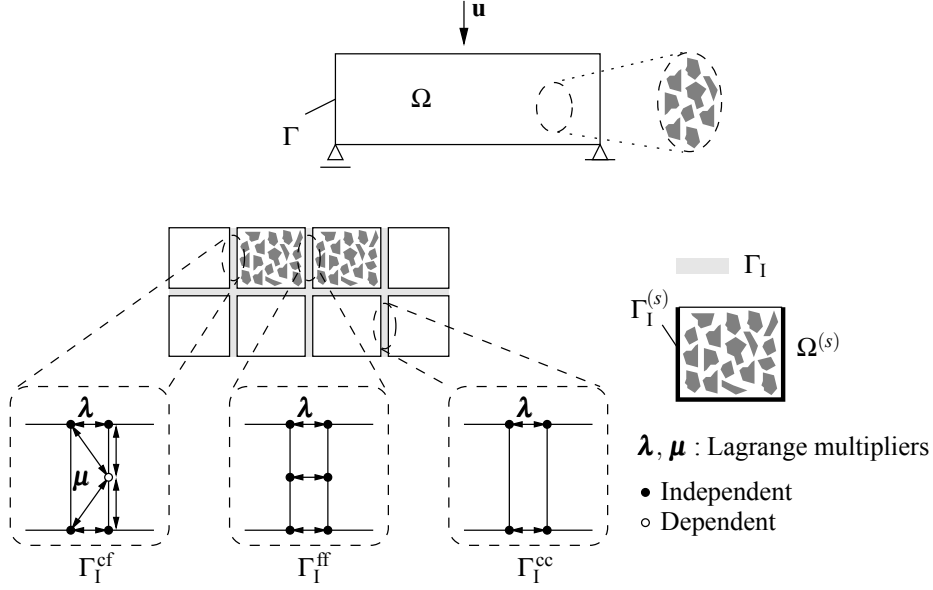
Figure 1: Beam with heterogeneous solid Ω (top). Decomposition in N_s domains (bottom).

dependent interface nodes as

$$\left[\begin{array}{ccc} \bar{\mathbf{B}}^{(1)} & \dots & \bar{\mathbf{B}}^{(N_s)} \end{array} \right] = \left[\begin{array}{ccc} \mathbf{B}^{(1)} & \dots & \mathbf{B}^{(N_s)} \\ \mathbf{C}^{(1)} & \dots & \mathbf{C}^{(N_s)} \end{array} \right]. \tag{2}$$

The matrices $\mathbf{B}^{(s)}$ correspond to the standard signed Boolean matrices of the FETI method while $\mathbf{C}^{(s)}$ contains the LMPC concerning dependent nodes.

Enforcement of the above mentioned continuity constraints is accomplished by the introduction of a heterogeneous Lagrange multiplier field

$$\delta\mathbf{\Lambda} = \left[\begin{array}{c} \delta\boldsymbol{\lambda} \\ \delta\boldsymbol{\mu} \end{array} \right] \tag{3}$$

in which $\delta\boldsymbol{\lambda}$ accounts for the independent nodes while $\delta\boldsymbol{\mu}$ represent the forces acting to constrain the dependent nodes.

The final linearized system of equilibrium equations for the decomposed solid with different resolutions can be written as

$$\left[\begin{array}{cccc} \mathbf{K}^{(1)} & \mathbf{0} & \mathbf{0} & \bar{\mathbf{B}}^{(1)\text{T}} \\ \mathbf{0} & \ddots & \mathbf{0} & \vdots \\ \mathbf{0} & \mathbf{0} & \mathbf{K}^{(N_s)} & \bar{\mathbf{B}}^{(N_s)\text{T}} \\ \bar{\mathbf{B}}^{(1)} & \dots & \bar{\mathbf{B}}^{(N_s)} & \mathbf{0} \end{array} \right] \left[\begin{array}{c} \delta\mathbf{u}^{(1)} \\ \vdots \\ \delta\mathbf{u}^{(N_s)} \\ \delta\mathbf{\Lambda} \end{array} \right] = \left[\begin{array}{c} \mathbf{f}_\text{ext}^{(1)} - \bar{\mathbf{B}}^{(1)\text{T}}\mathbf{\Lambda} - \mathbf{f}_\text{int}^{(1)} \\ \vdots \\ \mathbf{f}_\text{ext}^{(N_s)} - \bar{\mathbf{B}}^{(s)\text{T}}\mathbf{\Lambda} - \mathbf{f}_\text{int}^{(N_s)} \\ \mathbf{0} \end{array} \right], \tag{4}$$

where $\mathbf{K}^{(s)}, \mathbf{f}_\text{ext}^{(s)}$ and $\mathbf{f}_\text{int}^{(s)}$ refer to the tangent stiffness matrix, external and internal force vectors, respectively.

The augmented system in (4) is transformed into an interface flexibility problem following a standard FETI implementation [1].

2.2 Adaptive multiscale modeling

A multiscale analysis starts with a set of coarse scale domains with effective properties for the elastic bulk. Such effective properties can be computed with the use of classical homogenization theory [2] or numerical homogenization techniques [4, 14] on a Representative Volume Element (RVE) [3].

Adaptivity is accounted for by monitoring or anticipating the need for a highly detailed analysis at particular regions. Since our focus is directed to a study of crack growth and coalescence in brittle heterogeneous materials, a methodology is employed to anticipate the initiation of such phenomena and trigger a fine scale analysis in these particular regions. The resolution is upgraded domain-wise by mesh refinement when non-linearities are expected at domain $\Omega^{(s)}$. Consequently the interface tying relations need to be recomputed each time after a zoom-in. The reader is referred to the work in [13, 15] for a detailed formulation of strain/stress-based predictors for non-linear behaviour and zoom-in techniques for domain decomposition analysis.

3 STRONG AND WEAK MICRO-TO-MACRO CONNECTIONS

In the present approach, the interscale relations are defined employing a set of LMPC at non-conforming interfaces. These constraints enforce continuity of the incremental solution field $\delta\mathbf{u}(\mathbf{x})$ through the interface $\Gamma_\mathrm{I}^\mathrm{cf}$. A general weak form for such compatibility condition reads

$$\int_{\Gamma_\mathrm{I}^\mathrm{cf}} w(\mathbf{x})(\delta\mathbf{u}^\mathrm{f}(\mathbf{x}) - \delta\mathbf{u}^\mathrm{c}(\mathbf{x}))\,\mathrm{d}\Gamma_\mathrm{I}^\mathrm{cf} = \mathbf{0}, \quad \forall\mathbf{x} \in \Gamma_\mathrm{I}^\mathrm{cf}, \tag{5}$$
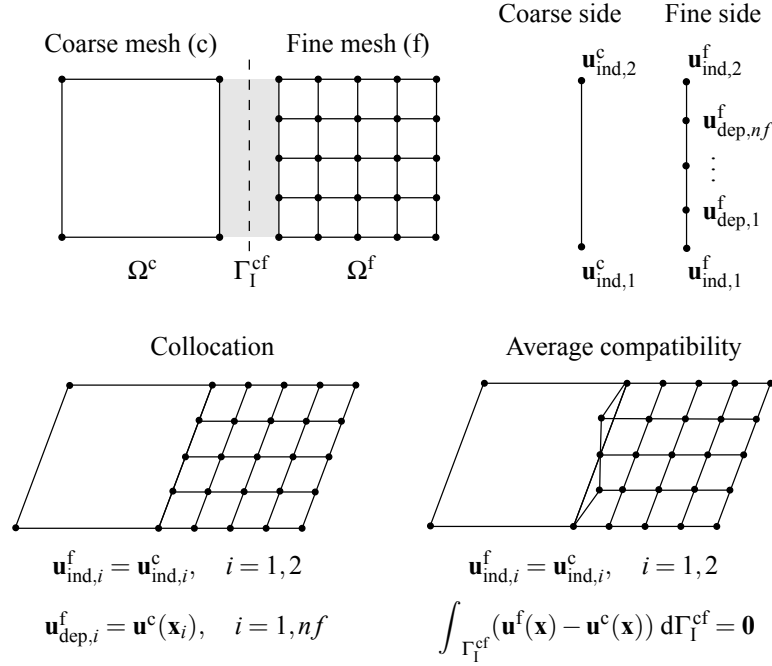
where $w(\mathbf{x})$ represents a weighting function. By setting $w(\mathbf{x})$ equal to the Dirac function $\delta(\mathbf{x})$ at all nodes, the standard collocation method is recovered. In this view the relations concerning independent (ind) and dependent (dep) nodes at the interface depicted in Figure 2 read

$$\mathbf{u}_{\mathrm{ind},i}^\mathrm{f} = \mathbf{u}_{\mathrm{ind},i}^\mathrm{c}, \quad i = 1, 2, \tag{6a}$$

$$\mathbf{u}_{\mathrm{dep},i}^\mathrm{f} = \mathbf{u}^\mathrm{c}(\mathbf{x}_i), \quad i = 1, nf. \tag{6b}$$

Note that the selection of linear or bilinear coarse scale elements leads to a linear distribution of the displacement field at the interface. Consequently, the resulting strains are constant at $\Gamma_\mathrm{I}^\mathrm{cf}$ between independent nodes. For this reason, such interscale relations present similarities with the constant strain approach typically adopted in classical homogenization theory.

Other choices of the weight function $w(\mathbf{x})$ lead to the so-called mortar methods [10]. In the present study, $w(\mathbf{x})$ is set to a constant which is an adequate choice for the case of

$$\mathbf{u}_{\text{ind},i}^{\text{f}} = \mathbf{u}_{\text{ind},i}^{\text{c}}, \quad i = 1, 2$$

$$\mathbf{u}_{\text{dep},i}^{\text{f}} = \mathbf{u}^{\text{c}}(\mathbf{x}_i), \quad i = 1, nf \qquad\qquad \int_{\Gamma_{\text{I}}^{\text{cf}}} (\mathbf{u}^{\text{f}}(\mathbf{x}) - \mathbf{u}^{\text{c}}(\mathbf{x})) \, d\Gamma_{\text{I}}^{\text{cf}} = \mathbf{0}$$

Figure 2: Strong and weak micro-macro connections.

linear shape functions as argued in [12]. The resulting relations are referred to as average compatibility in the remaining of the text and read

$$\mathbf{u}_{\text{ind},i}^{\text{f}} = \mathbf{u}_{\text{ind},i}^{\text{c}}, \quad i = 1, 2, \tag{7a}$$

$$\int_{\Gamma_{\text{I}}^{\text{cf}}} (\mathbf{u}^{\text{f}}(\mathbf{x}) - \mathbf{u}^{\text{c}}(\mathbf{x})) \, d\Gamma_{\text{I}}^{\text{cf}} = \mathbf{0}. \tag{7b}$$

The set of constraints in (7) enforce continuity of the solution field in a weak sense for the interface segment bounded by the independent nodes, the independent nodes satisfying the strong compatibility (7a). This can be adequate when the fine scale solution field at the interface cannot be properly captured with the coarse scale shape functions. For this reason there is a gain in flexibility at the non-conforming interface. Note that the weak constraint in (7b) is obtained by choosing a constant distribution of Lagrange multipliers $w(\mathbf{x})$ in the standard weak form of interface compatibility used in the FETI method. In this view, the interscale relation based on average compatibility preserves some similarities with the constant stress assumption in the classical homogenization theory.

Besides the nature of strong and weak compatibility constraints, the number of equations involved in (6) and (7) are significantly different. Enforcement of collocation constraints (6b) at the interface $\Gamma_{\text{I}}^{\text{cf}}$ requires a set of $nf \times N_{\text{dof}}$ equations (refer to Figure 2), nf being the number of dependent nodes and N_{dof} the number of degrees of freedom per node. However, the number of equations concerned in (7b) is N_{dof}. Both collocation and
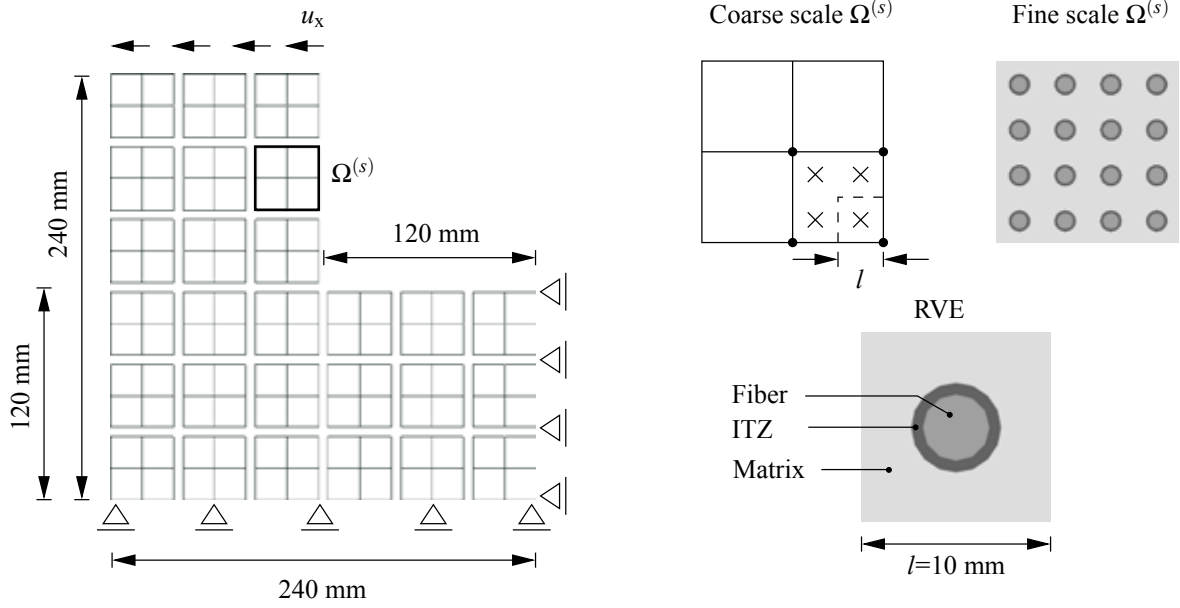
Figure 3: Set-up of the multiscale domain decomposition analysis.

average compatibility constraints can be cast in a matrix form for each domain $\Omega^{(s)}$ as

$$\mathbf{C}^{(s)}\mathbf{u}^{(s)} = \mathbf{0}. \tag{8}$$

The matrices $\mathbf{C}^{(s)}$ are used in the assembly of the modified Boolean matrices $\bar{\mathbf{B}}^{(s)}$ as shown in (2). Since the number of rows of $\mathbf{C}^{(s)}$ depends on the micro-to-macro connection method, the size of the resulting interface problem becomes lower for the choice of average compatibility constraints.

4 EXAMPLES

A multiscale analysis of an L-shape specimen with heterogeneous mesostructure is performed using the presented domain decomposition framework. The specimen is meshed using a coarse discretization and partitioned into 27 non-overlapping domains. The underlying heterogeneous structure consists of a number of regularly distributed steel fibers. Computations are performed considering a two-dimensional slice of the structure in which plane strain conditions are assumed. The regular distribution of fibers allows the retrieval of effective elastic properties from a simple unit cell which is treated as an RVE. The problem set-up is summarized in Figure 3. Non-linear behaviour is linked to crack nucleation and propagation in our study and is simulated by means of a gradient-enhanced damage model [16]. Tensile failure is modeled adopting a Mazars [17] definition for the equivalent strain $\tilde{\varepsilon}$. An exponential evolution of damage ω with the maximum strain κ is considered. A summary of the material parameters is given in Table 1. The non-local equivalent strain $\tilde{\varepsilon}_{\mathrm{nl}}$ is adopted as the internal variable invariant used to construct the

	Material parameters		Soft inclusion	Matrix	Coarse bulk
E	Young's modulus	[N/mm^2]	20.0×10^2	40.0×10^3	Effective
ν	Poisson's ratio	[−]	0.2	0.2	Effective
$\tilde{\epsilon}_{\mathrm{nl}}$	Non-local equivalent strain	[−]	Mazars	Mazars	Mazars
κ_0	Damage initiation threshold	[−]	5.0×10^{-5}	8.5×10^{-5}	5.0×10^{-5}
c	Gradient parameter	[mm^2]	1.5	1.5	1.5
$\omega(\kappa)$	Damage evolution law	[−]	Exponential	Exponential	[−]
α	Residual stress parameter	[−]	0.999	0.999	[−]
β	Softening rate parameter	[−]	400	400	[−]

Table 1: Material parameters.
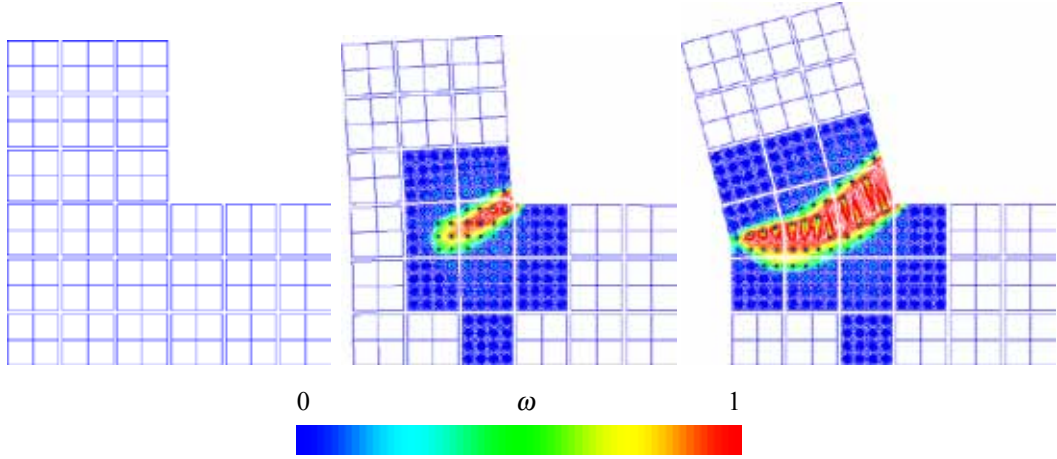
Figure 4: Evolution of damage growth during multiscale analysis.

non-linear domain predictor [13]. Upon increasing load, damage grows and propagates from the re-entrant corner of the L-shape specimen as shown in Figure 4. The interscale relations used in this analysis correspond to the collocation constraints (6). Due to the adaptive nature of the interface it is possible to capture the development of non-linearity satisfying continuity of the solution throughout the complete specimen.

The load-displacement curves depicted in Figure 5 show the sensitivity of the method to different elastic effective properties for the coarse bulk. In these tests, collocation is adopted at $\Gamma_{\mathrm{I}}^{\mathrm{cf}}$ and the effective elastic moduli are retrieved by classical homogenization, i.e. Voigt, Reuss and Mori-Tanaka averaging schemes, and computational homogenization, i.e. fully prescribed forces, displacements and periodic boundary conditions. All multiscale analyses (gray area) are plotted together with the direct numerical solution (DNS). The agreement between multiscale analyses and DNS depends on the choice of effective elastic properties for the coarse bulk. The differences between multiscale analysis and DNS are higher in the pre-peak region since the overall behaviour is dominated by the chosen effective elastic properties. However, in the post-peak region, these differences
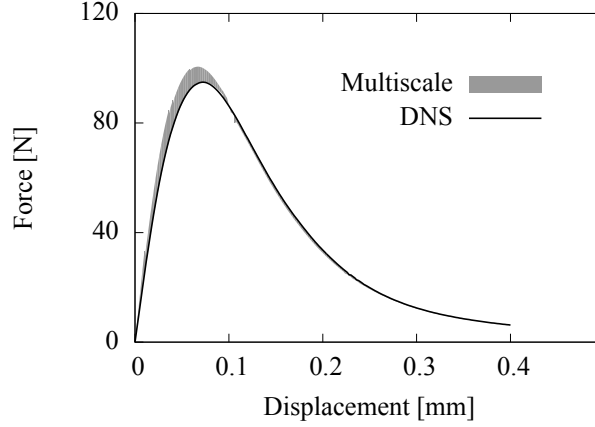
Figure 5: Load-displacement curves for the DNS and multiscale analysis.

become smaller due to the fact that non-linear areas are fully considered.

An assessment of collocation and average compatibility interscale relations is carried out by comparing the damage field between multiscale analysis and DNS at ultimate loading stage (Figure 9). The absolute error in ω is defined as

$$E_\omega = |\omega_{\mathrm{DNS}}| - |\omega_{\mathrm{Mult}}|, \quad 0 \le E_\omega \le 1. \tag{9}$$

A small increase of E_ω is observed for the average compatibility constraint although differences remain in an acceptable range. The error E_ω is higher around the domain interfaces where a steep damage gradient needs to be captured. The overall cost of the interscale relation in the multiscale analysis is found by computing the size of the interface problem (Figure 7). The active interface is defined as the ratio between the number of degrees of freedom involved in the interface Γ at load step t and the maximum number obtained by considering all fine scale domains. In both collocation and average compatibility the active interface grows with the activation of fine scale domains. However, the interscale relations based on average compatibility constraints lead to a lower active interface and this has a beneficial impact on the overall cost of the analysis.

5 CONCLUSIONS

A multiscale domain decomposition framework for the analysis of heterogeneous quasi-brittle materials is presented. The multiscale strategy provides results which are in agreement with a reference DNS and results in a much lower computational cost. The analyses are influenced by the choice of the effective elastic properties for the coarse bulk and the micro-to-macro connection strategy. The tests performed on a steel reinforced L-shape specimen reveal that both interscale relations give similar results although the accuracy is higher for the collocation constraint. However, average compatibility techniques provide a cheaper overall cost which might be preferred in large scale computations.
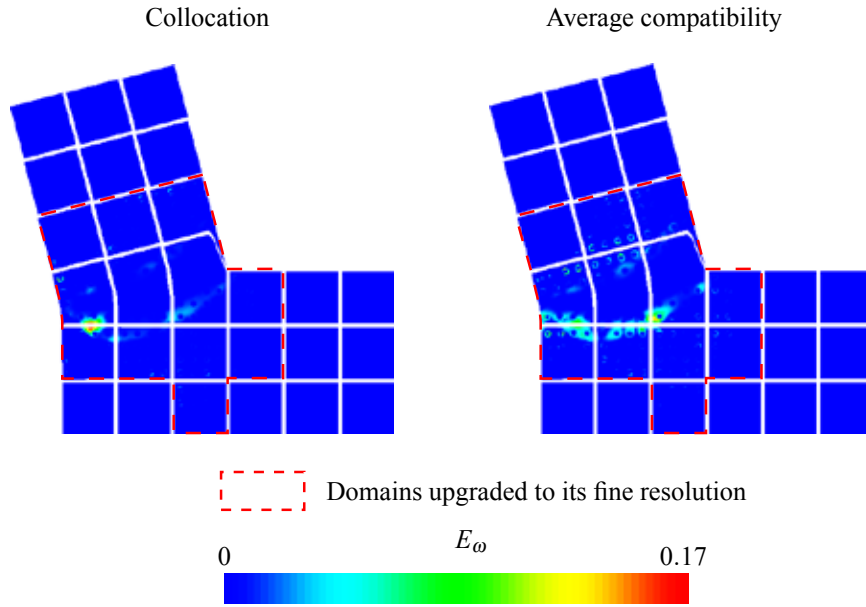
Figure 6: Damage field error E_ω between DNS and multiscale analyses.
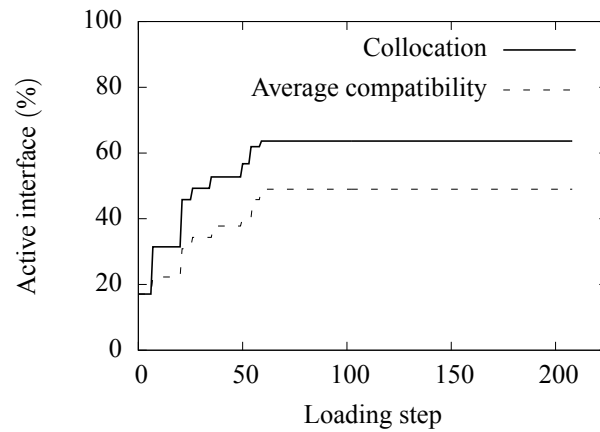
Figure 7: Evolution of the size of the interface problem.

REFERENCES

[1] C. Farhat and F. X. Roux. A method of finite element tearing and interconnecting and its parallel solution algorithm. *International Journal for Numerical Methods in Engineering*, 32(6):1205–1227, 1991.

[2] S. Nemat-Nasser and M. Hori. *Micromechanics: Overall properties of heterogeneous materials.* North-Holland, 1993.

[3] R. Hill. Elastic properties of reinforced solids: Some theoretical principles. *Journal of the Mechanics and Physics of Solids*, 11(5):357–372, 1963.

[4] H. Moulinec and P. Suquet. A numerical method for computing the overall response of nonlinear composites with complex microstructure. *Computer Methods in Applied Mechanics and Engineering*, 157(1-2):69–94, 1998.

[5] F. Feyel and J. L. Chaboche. FE^2 multiscale approach for modelling the elastoviscoplastic behaviour of long fibre SiC/Ti composite materials. *Computer Methods in Applied Mechanics and Engineering*, 183(3-4):309–330, 2000.

[6] V. Kouznetsova, W. A. M. Brekelmans, and F. P. T. Baaijens. An approach to micro-macro modeling of heterogeneous materials. *Computational Mechanics*, 27(1):37–48, 2001.

[7] T. J. R. Hughes, G. R. Feijóo, L. Mazzei, and J. B. Quincy. The variational multiscale method–a paradigm for computational mechanics. *Computer Methods in Applied Mechanics and Engineering*, 166(1-2):3–24, 1998.

[8] A. Hund and E. Ramm. Locality constraints within multiscale model for non-linear material behaviour. *International Journal for Numerical Methods in Engineering*, 70(13):1613–1632, 2007.

[9] P. Ladevèze, O. Loiseau, and D. Dureisseix. A micromacro and parallel computational strategy for highly heterogeneous structures. *International Journal for Numerical Methods in Engineering*, 52(12):121–138, 2001.

[10] C. Bernardi, Y. Maday, and A. Patera. A new nonconforming approach to domain decomposition: The mortar element method. In H. Brezis and J. L. Lions, editors, *Nonlinear Partial Differential Equations and Their Application*, Pitman, 1989.

[11] F. B. Belgacem. The mortar finite element method with lagrange multipliers. *Numerische Mathematik*, 84(2):173–197, 1999.

[12] A. Mobasher Amini, D. Dureisseix, and P. Cartraud. Multi-scale domain decomposition method for large-scale structural analysis with a zooming technique: Application to plate assembly. *International Journal for Numerical Methods in Engineering*, 79(4):417–443, 2009.

[13] O. Lloberas-Valls, D. J. Rixen, A. Simone, and L. J. Sluys. Domain decomposition techniques for the efficient modeling of brittle heterogeneous materials. *Computer Methods in Applied Mechanics and Engineering*, 200(13–16):1577–1590, 2011.

[14] C. Miehe and A. Koch. Computational micro-to-macro transitions of discretized microstructures undergoing small strains. *Archive of Applied Mechanics*, 72(4):300–317, 2002.

[15] O. Lloberas-Valls, D. J. Rixen, A. Simone, and L. J. Sluys. Multiscale domain decomposition analysis of quasi-brittle heterogeneous materials. *International Journal for Numerical Methods in Engineering*, 2010. (Submitted, October 19, 2010).

[16] R.H.J. Peerlings, R. de Borst, W. A. M. Brekelmans, and J.H.P. de Vree. Gradient enhanced damage for quasi-brittle materials. *International Journal for Numerical Methods in Engineering*, 39(19):3391–3403, 1996.

[17] J. Mazars and G. Pijaudier-Cabot. Continuum damage theory–application to concrete. *Journal of Engineering Mechanics*, 115(2):345–365, 1989.